Hot carrier transfer in graphene/PtSe$_2$ heterostructure tuned by built-in electric field

Qiushi Ma[1,2], Wenjie Zhang[3], Chunwei Wang[2,4], Ruihua Pu[2], Chengwei Ju[5], Xian Lin[3], Zeyu Zhang[4*], Weiming Liu[2*], and Ruxin Li[2,4]

[1] School of Resource and Environmental Engineering, Hefei University of Technology, Hefei 230009, Anhui Province, China

[2] School of Physical Science and Technology, ShanghaiTech University, Shanghai 201210, China

[3] Department of Physics, Shanghai University, Shanghai 200444, China

[4] State Key Laboratory of High Field Laser Physics and CAS Center for Excellence in Ultra-intense Laser Science, Shanghai Institute of Optics and Fine Mechanics (SIOM), Chinese Academy of Sciences (CAS), Shanghai 201800, China

[5] College of Chemistry, Nankai University, Tianjin 300071, China

[*] Corresponding Authors, zhangzeyu@siom.ac.cn (Z.Zhang), liuwm@shanghaitech.edu.cn (W. Liu)

ABSTRACT

Van der Waals heterojunction involving graphene (Gr) with transition metal dichalcogenides (TMDs) is regard as a promising structure for their outstanding performance in optical and optoelectronic response. The electron-hole thermalization has been deemed to be the main reason for the sub-bandgap-excitation charge transfer from Gr to TMDs. However, the role of the intricate interlayer interaction of the Gr and the TMDs still require intensive investigation. Here, we have investigated the photocarrier dynamics in 5-layer $PtSe_2$/Gr heterojunction by using time-resolved optical pump and terahertz probe spectroscopy. Interestingly, after photoexcitation, electron transfer from $PtSe_2$ to Gr in $PtSe_2$/Gr/substrate heterojunction has been demonstrated successfully, by contrast, no observable charge transfer occurs in the Gr/$PtSe_2$/substrate heterostructure. The prominent difference for the different stacking sequence between Gr and $PtSe_2$ can be ascribed to the effective built-in field introduced by fused silica substrate. A physical picture accounting for built-in electric field introduced by substrate has been proposed to interpret the charge transfer process in the TMD/Gr heterostructure–the substrate built-in electric field plays a dominated role for controlling the charge transfer pathway in the TMDs/Gr heterojunction. This study not only shed the light to the substrate engineering but also provide a new insight into the dynamic in Gr/TMDs heterojunction, which provides a new method to optimize the performance of photodetection.

Keywords: built-in electric field, Charge transfer, Time-resolved THz spectroscopy, TMDs, graphene

Introduction

Two-dimensional (2D) materials including graphene, monolayer TMDs (MoS_2, $MoSe_2$, WS_2, WSe_2 etc.) have captured great attention due to their potential applications in optics[1-2], electronics[3], optoelectronics[4-5], and electrochemicals[6-7]. With the novel characteristics comparing with bulk materials, 2D materials provide opportunities to design desired optical and optoelectronic device with new functionalities.[8] A class of van der Waals heterojunction structure–artificially stacking layers with different kinds of 2D materials, representing a new class of 2D materials.[9-11] In contrast to traditional semiconductor, in which the heterojunction can be formed under lattice matching condition only, lattice mismatch can be ignored when stacking different 2D materials into heterojunction, thus providing a platform for improving the photoactive applications and further understanding the carrier dynamics in 2D materials.[12-13] Many heterojunctions have been designed and fabricated such as Gr/TMDs in recent years.[4, 9, 12, 14-16] Manipulation of charge transfer across the interfaces provides atomically-thin-heterojunction potential materials in replacing the traditional optoelectronics.

Among many heterostructures, the Gr/TMDs heterojunction has been paid special attention due to the easy fabrication, tunable Fermi surface of graphene, high conductivity, as well as efficient charge transfer across the interface between two materials.[17-19] Additionally, due to the efficient thermalization within the electronic system in graphene, hot carriers in graphene after photoexcitation can inject into the TMDs even photon energy is well below the band gap of the TMDs.[16, 18, 20] In WS_2/Gr bilayer heterojunction, different physical pictures are proposed. By using transient absorption micro-spectroscopy combined with DFT calculation, Yuan $et. al.$ reported that the excitation below WS_2 bandgap and leading to enhancement in photocarrier generation by visible optical excitation.[16] Chen $et. al.$ demonstrated high efficiency (~50%) carrier injection from graphene into WS_2 via transient absorption spectroscopy, and they proposed a 2μPTE model,[21] in which the photoexcited electrons and holes establish separate Fermi distribution with electrons in conduction band and hole in valence band in undoped graphene within sub-picosecond time scale.

Fu *et. al.* came out that hot electron transfer occurs upon photon energy below the A-exciton,[18] while hole transfer takes place upon above A-exciton photoexcitation, and the experiment results are well reproduced by the phenomenological thermodynamic model.[18] All these proposed models can well explain the carrier transfer in the individual Gr/TMD heterostructure, but few studies investigate the influence of the stacking order between Graphene and TMDs on the charge transfer and carriers dynamic as far as we learn about.[19]

Besides the attractive and interesting dynamics of carriers in Gr/TMDs heterojunction, the substrate effect can have great impact on the charge transfer in the heterojunction as well, which has been paid little attention in previous studies.[19, 22] Owing to weak coupling between TMD and graphene interface, the electronic states of participating materials remain largely unchanged. With the external electric field induced by substrate, charge transfer process in the heterojunction is manageable by substrate engineering. Xing *et. al.[19]* reported the impact of built-in field introduced by sapphire substrate on the charge transfer process between WSe_2/Gr via optical pump and THz probe and transient absorption spectroscopy. Moreover, previous theoretical studies have pointed out that the built-in field can have important influence on the charge transfer in TMD heterojunction[23], this arises our interests that how important of the built-in electric field is for the charger transfer process in Gr/TMDs heterojunction.

In this article, by employing optical pump and THz probe (OPTP) spectroscopy, we have investigated the charge transfer process in a 5-layer $PtSe_2$/Gr heterojunction on a fused silica substrate. The experimental results demonstrate that ultrafast charge injection from $PtSe_2$ to graphene occurs after photoexcitation, and the charge injection process is strongly related to the built-in electric field introduced by substrate. In $PtSe_2$/Gr/substrate, the substrate built-in electric field is pointed from Gr layer to $PtSe_2$ layer, the photoexcited electrons transfer process is promoted leading to negative THz photoconductivity under low pump fluence. With increasing the pump flunece, the negative THz photoconductivity develop into positive one gradually due to the screening of built-in field by the photogenerated carriers, which precludes the occurrence of charge transfer. By increasing the pump fluence further, the

heterostructure exhibits positive THz photoconductivity arising from photocarriers of $PtSe_2$ solely, in which the built-in electric field has been screened completely by photocarriers. In contrast, no observable charges transfer in $Gr/PtSe_2$/substrate occurs because the built-in electric field hinders the electron injection process, in which the THz photoconductivity remains positive under various pump fluences and excitation wavelengths. Our experimental results in $Gr/PtSe_2$ heterostructures provide solid evidence that the driving force for the occurrence of charge transfer is dominated by built-in field introduced by substrate rather than pumping photoenergy.

Experimental section

Large-area monolayer graphene and 5-layer (5L) $PtSe_2$ heterostructures on 1 mm-thick fused silica substrate were grown by chemical vapor deposition method (provided by six-carbon technology, Shenzhen China). Two samples with different stacking order were fabricated, $PtSe_2$/Graphene/substrate was named as G1 and Graphene/$PtSe_2$/substrate was named as G2 in the left part of this article.

Time-resolved THz spectroscopy was performed using a 120 fs, 1 kHz Ti: Sapphire regenerative amplifier system. The THz pulses were generated and detected with a pair of 1 mm-thick, (110)-oriented ZnTe crystals. The wavelength tunable pump pulse is delivered from optical parameter amplifier system (TOPAS-C) pumped with 800 nm pulse. The spot size on the sample was 3 mm for the THz beam and 6.5 mm for the pump beam. We measured the pump-induced THz electric field transmission (ΔE) normalized to the THz transmission without photoexcitation (E_0) for the same sample as a function of the pump–probe delay t. All measurements were performed at room temperature.

Results and discussions

Figure 1(a) illustrates the side view of the $Gr/PtSe_2$ heterojunction, which is constructed from the CVD growth monolayer graphene and 5-layer $PtSe_2$ on a fused silica substrate. Figure 1(b) shows UV-vis absorption spectra of the two heterostructures with different stacking order. According to the previous report, $PtSe_2$ film changes from semiconductor into semimetal with the increasing thickness.[24-25] The band gap of our 5-layer $PtSe_2$ is determined to be about 0.52 eV from the

UV-visible absorption spectra, which is accord to the previous report.[24] Both G1 and G2 show similar absorption and identical bandgap.[25] A typical Raman spectrum obtained from two heterojunctions are demonstrated in Fig. 1(c). The inset in Fig. 1(c) shows two pronounced peaks in 175 cm^{-1} and 204 cm^{-1}. The peaks in the two films can be ascribed to in-plane vibration (175 cm^{-1}, E_g mode) and out of plane vibration (204 cm^{-1}, A_{1g} mode) of the Pt and Se atoms,[24] respectively. The intensity rations of A_{1g} and E_g is about 0.16 that is nearly same as previous report.[25] Intriguingly, two obvious peaks in Fig. 1(c) are contributed by G-band and D-band of monolayer Graphene.[26-27] The Raman spectra and transient THz spectroscopy indicates the graphene in our heterostructure is n-type. The position of the G-band in G1 (1591 cm^{-1}) shows a large blue shift with that of G2 (1583 cm^{-1}), which indicates different carrier concentration in the two heterostructures. The central frequency of G-band can be used to estimate the Femi level by $E_F = (\nu_G - 1580 \text{ cm}^{-1})/42 \text{ cm}^{-1}\text{eV}^{-1}$.[28] The Femi level in G1 is calculated about 0.2 eV and the Fermi energy in G2 is much close to the Dirac point than that in G1. The prominent difference in the graphene Fermi level with different stacking order can be ascribed to the effect of built-in electric filed induced by substrate. The built-in field in G1 heterostructure points from graphene to PtSe$_2$, which enable electron charges in PtSe$_2$ tend to move towards graphene. In contrast, the effect of built-in field in G2 tends to move electrons out of graphene. In short, the experimental results demonstrate substrate induced built-in electric field has great impact on the Fermi energy of graphene for different stacking sequence of Gr/PtSe$_2$ heterostructures.
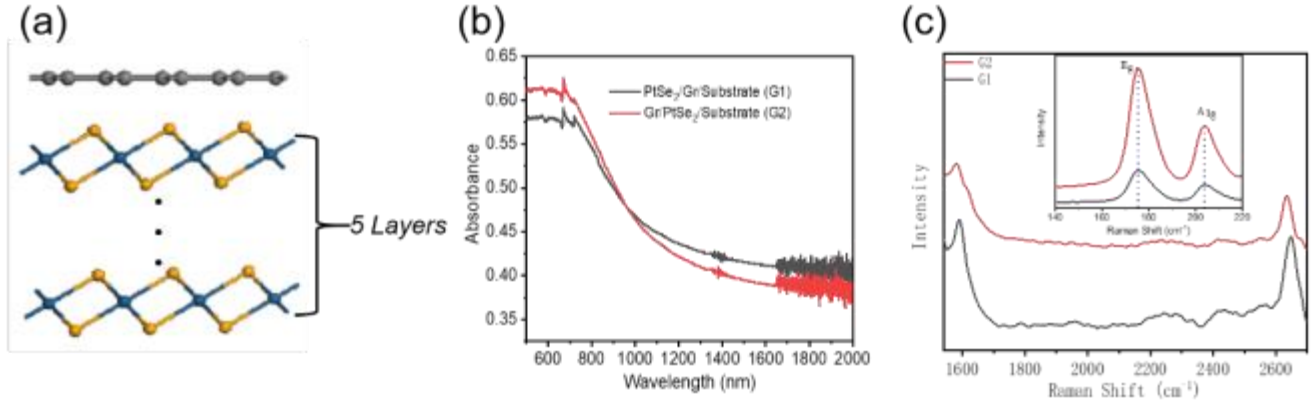
Fig. 1 (a) Schematic of the heterostructures for 5L-PtSe$_2$ /Gr from the side view. (b) UV-visible absorption spectra of G1 (black) and G2 (red). (c) Raman spectra of G1 (black) and G2 (red). The inset plots the Raman spectra of E$_g$ and A$_{1g}$ modes of PtSe$_2$. For comparison, UV-visible absorption and Raman scattering spectra of silica substrate supported 5-layer PtSe2 film are presented in Fig. S1 in Supplementary Information (SI)

To further explore the dynamical charge transfer in the two heterostructures with photoexcitation, OPTP spectroscopy is employed to study the photocarrier dynamic at room temperature. The carrier dynamic of 5L PtSe$_2$ is also studied by OPTP as well for comparison. For the film with thickness of a few nm, $\Delta E/E_0$ is related to the photoinduced sheet conductivity, $\Delta\sigma$, which is[29]

$$\sigma = \qquad\qquad\qquad \text{(Eq. 1)}$$

Where n=1.95 is the refractive index of the fused silica substrate, and Z$_0$=377 is the free space impedance.[19] Figure 2 shows the transient THz photoconductivity (-$\Delta E/E_0$) of G1 heterostructures under 780 nm (a) and 1300 nm (b) with various pump fluences. Interestingly, the THz photoconductivity is negative at low pump fluence but develops into positive signal with increasing pump fluence gradually at both excitation wavelengths. Phenomenally, the pump fluence dependent THz photoconductivity shown in Figs. 2(a) and (b) can be divided into three regime: (i) all the THz photoconductivity signals remain negative at low pump fluence; (ii) all signals remain positive under high fluence; (iii) the signal contains both positive at earlier delay time and negative signal at later delay time under intermediate fluence. For comparison,

the transient THz response of 5L PtSe$_2$ film on fused silica substrate under identical photoexcitation at 780 nm is presented in Fig. S2 in SI. It is noted that the 5-layer PtSe$_2$ film always shows positive THz photoconductivity and monolayer graphene demonstrates negative THz photoconductivity. The THz photoconductivity for both PtSe$_2$ and graphene films alone does not change sign with various pump fluences. In addition, it should be noticed that the THz photoconductivity of individual 5L PtSe$_2$ is at least 5 times larger than that of monolayer graphene under identical photoexcitation at both 780 nm and 1300 nm. Therefore, if there is no charge transfer between two materials, the THz photoconductivity should keep positive under all conditions. In fact, the heterostrucutre behaves negative signal under low pump fluence, which manifests that transient THz response from graphene plays dominated role under low pump fluence, and charge transfer across the interface is expected to occur in the heterostructures after photoexcitation. Let's discuss the photoinduced negative signal first, as illustrated in the inset of Figs. 2(a) and (b), the magnitude of negative signal increases with pump fluence less than 25 mJ/cm^2 for both 780 and 1300 nm. Considering much higher Fermi level (~0.2 eV) of graphene in G1 heterosructure as well as the relatively lower pump fluence, the negative THz photoconductivity in G1 is ascribed to the efficient intra-band scattering in graphene that heats electron to high temperature, leading to faster momentum scattering time, and therefore decrease the THz photoconductivity according to Drude model.[27, 30-31] The elevated electron temperature is achieved under higher pump fluence, which cause larger negative THz photoconductivity in graphene. The OPTP signal under low pump fluence in our G1 heterojunction is accord to the graphene response. The positive THz photoconductivity signal under high pump fluence is dominated by PtSe$_2$. The red dots in the insets of Fig. 2 (a) and (b) plot the peak value of THz photoconductivity (i.e. (-DE/E$_0$)$_{max}$) with respect to the pump fluence, which are accord to that of 5L PtSe$_2$ as shown in Fig. S2 in SI. We then pay attention to the THz photoconductivity that shows both positive and negative signals under intermediate pump fluence. With increasing pump fluence, the negative signals become weaker and disappear finally, while the positive signal becomes more pronounced and plays dominated role under

higher pump fluence. In conclusion, our pump fluence dependent THz photoconductivity in G1 heterostructure shown in Figs. 2(a) and (b) demonstrates that the negative THz photoconductivity under low pump fluence is accord to thermalized carriers in graphene, which are photoinjected from PtSe$_2$. While the positive THz photoconductivity under high pump fluence is accord to the photocarriers response in PtSe$_2$, in which the carriers transfer process is precluded and the photoexcitation of PtSe$_2$ plays the dominated role. Under intermediate pump fluence, the THz photoconductivity response in G1 could be the superposition of transient THz response of monolayer graphene and that of 5L PtSe$_2$.
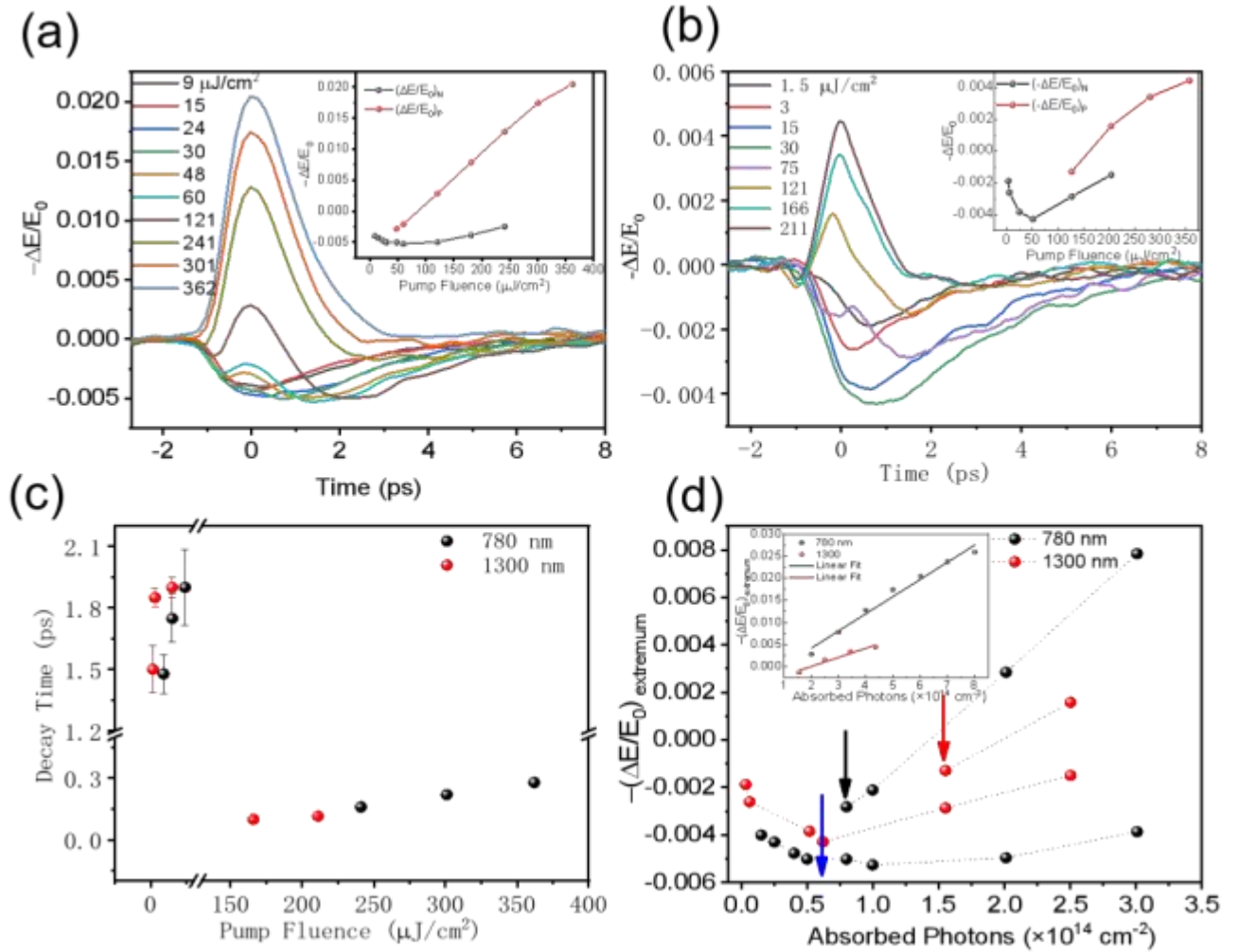

Figure 2 (a and b) The transient THz photoconductivity of G1 under various pump fluence excited by (a) 780 nm and (b) 1300 nm. The inset plots the peak modulation depth, $-\Delta E/E_0$ with respect to the pump fluence for the two excitation wavelengths. (c) The pump fluence dependent relaxation

time of photoconductivity in G1 under low (less than 25 mJ/cm^2) and high pump fluence (higher than 150 mJ/cm^2) at 780 nm (black) and 1300 nm (red), respectively. (d) The extracted extremums of THz photoconductivity with respect to absorbed photon density with low and intermediate pump fluence for the excitation wavelength of 780 nm (black) and 1300 nm (red). The arrows in blue, black and red indicate the minimum magnitude of $\Delta\sigma$, the thresholds of two THz photoconductivity extremums at 780 and 1300 nm, respectively. Inset plots the magnitude of $\Delta\sigma_{max}$ with respect to absorbed phonon density at high pump fluence for 780 and 1300 nm excitation.

In order to better understand the dynamics of the charge transfer, we employed a phenomenological model to fit the dynamics of photoconductivity by Eq. 2 as follows

$$-\frac{\Delta E}{E_0} = A * \exp\left[\left(\frac{\omega}{\tau}\right)^2 - \frac{t}{\tau}\right] * \Bigg[\qquad \text{(Eq. 2)}$$

Where t is the pump-probe delay time, τ and A are the correlative relaxation constant and amplitude, respectively. w is the THz probe pulse. Figure 2(c) displays the pump fluence dependent relaxation time for both negative THz photoconductivity at low pump fluence and positive THz photoconductivity at high pump fluence. It can be adopted that, with increasing pump fluence, the relaxation time increases under low pump fluence scope, and it is noted that the relaxation of negative signal is strongly relevant to the pump fluence for both wavelengths as shown in Fig. 2(c), which indicates again that the negative signal is accord to the photoresponse of graphene.[26, 32] The transient negative THz photoconductivity response also shows a good agreement with the prediction of thermodynamics model of graphene.[27, 31] Our results reveal that the photocarrier dynamics of graphene plays dominant role at low pump fluence scope. Additionally, as seen from Figure 2(c), the relaxation time of positive photoconductivity under 780 nm (black) and 1300 nm (red) excitation shows a clear trend: the relaxation time increases with pump fluence. This implies that the positive signal is accord to PtSe$_2$, which indicates that high pump fluence could block the charge transfer process from PtSe$_2$ to graphene. As a result, most of photocarriers are

populated in PtSe$_2$ layer leading to the positive THz photoconductivity.

If the photoinduced charge transfer takes place in the G1, it should also appear in G2 heterostruture as well. However, the photoconductivity remains positive under various pump fluence at both wavelengths of 780 and 1300 nm as shown in Fig. 3. The pump fluence and photon energy independence of transient THz response in G2 suggests that the positive THz photoconductivity mainly comes from the PtSe$_2$ layer, which indicates that no charge transfer occurs in G2 heterostructure. The inset in Fig. 3 plots the peak THz photoconductivity with respect to pump fluence for excitation wavelengths of 780 nm (a) and 1300 nm (b). It is seen that pump fluence dependent THz photoconductivity of G2 at both excitation wavelengths shows almost same as that of 5L PtSe$_2$ film. This arises our interest what cause the difference of THz photoconductivity in the two films. A built-in field model has been proposed to explain the phenomenon.
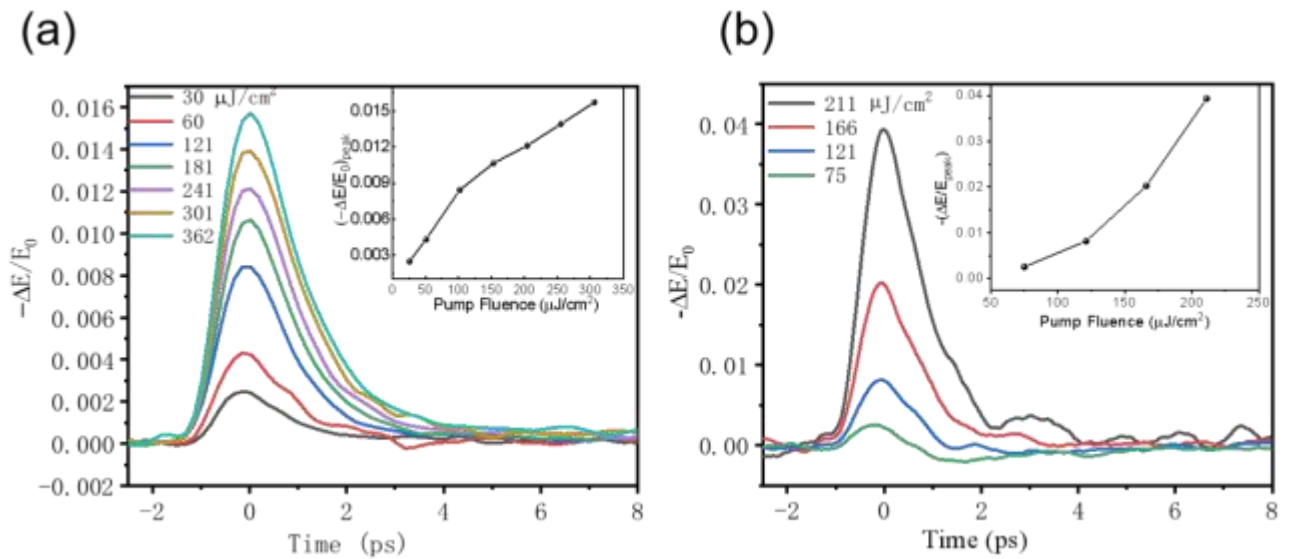

Fig. 3 The transient THz photoconductivity of G1 under various pump fluence excited by (a) 780 nm and (b) 1300 nm. The inset plots the peak modulation depth, $\Delta E/E_0$ with respect to the pump fluence.

The experimental results shown in Fig. 2 demonstrate that the stacking order of PtSe$_2$

and graphene has great impact on the carrier dynamic. Many studies have shown that electric field is induced by different substrates, and theoretical calculation reveals that the electric field can promote/preclude the carrier injection between Gr/TMDs heterojunction after photoexcitation.[23, 33] The electric field introduced by substrate always points outside the substrate surface. In our $PtSe_2$/Gr heterojunction, it can be well explained by substrate induced built-in electric field as well. The built-in electric field introduced by silica substrate is in favor of charge transfer in G1 after photoexciation.[19] By contrast, charge transfer from $PtSe_2$ to graphene is prevented in the G2 heterostructure considering the direction of the built-in electric field introduced by substrate.

In order to exhibit the importance of the built-in electric field on the charge transfer process in G1, Figure 2(d) plots the extremum of THz photoconductivity with respect to the absorbed photon density extracted from Figs. 2(a) and (b), respectively. It can be seen that the THz photoconductivity with respect to absorbed photon density shows two extremums: a positive one from $PtSe_2$ and negative one from graphene, and we assign this this phenomenon as the screening of built-in electric field by photogenerated carriers. Interestingly, the screening of electric field starts to take visible effect around 1.55×10^{14} cm^{-2} (red arrow in Fig. 2(d)) for 1300 nm, which is about 2-fold of that for 780 nm excitation (0.8×10^{14} cm^{-2}, (black arrow in Fig. 2(d))). Since the screening of electric field starts to appear at much lower photon density for 780 nm than 1300 nm, the saturation of charge transfer cannot be dominated by Pauli blocking effect. It should be noted that the carrier multiplication occurs under 780 nm excitation, which can be clearly seen from the inset in Fig. 2(d). The magnitude of ($-DE/E_0)_{max}$ with respect to absorbed photon density can be well reproduced with linear function, and the slope at 780 nm excitation is twice as that of 1300 nm.
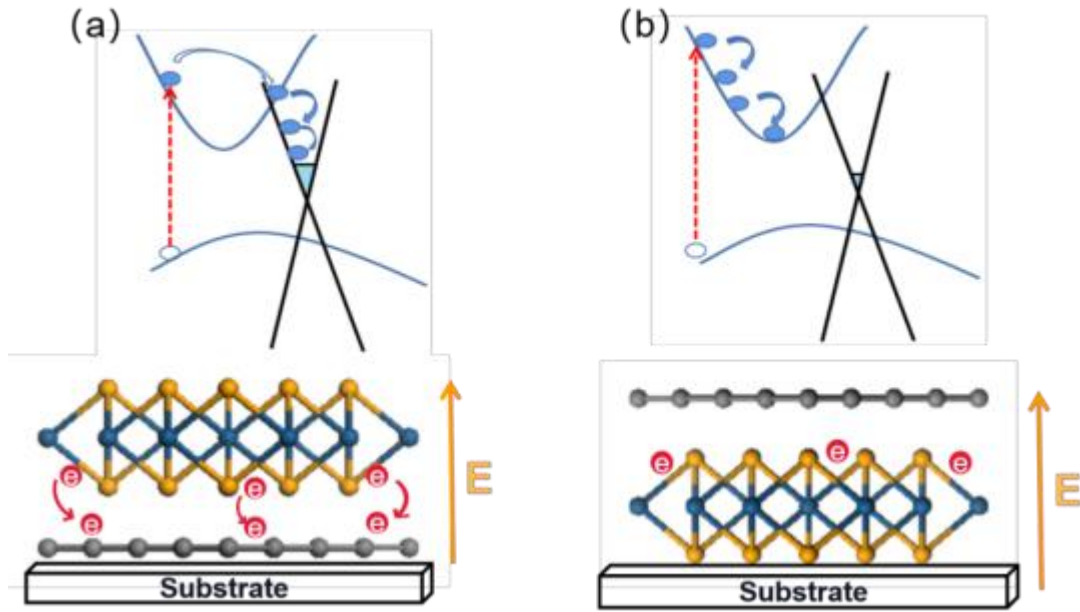
Figure 4. (a) Schematic diagram of the photophysical processes in G1 heterostructure under photoexcitation (top (a)) as well as the influence of effective field introduced by substrate (bottom (a)). (b) Schematic illustrations of the photophysical process in G2 heterostructure under photoexcittion (top (b) as well as the influence of effective field introduced by substrate (bottom (b)).

The physical pictures of photoinduced charge transfer as well as the effect of substrate in Gr/PtSe$_2$ heterostrucutre are depicted in Fig. 4(a) and 4(b), respectively. For the G1 heterostrucutre illustrated in Fig. 4(a), built-in field introduced by substrate promote the charge transfer process after photoexcitation: under low pump fluence, the photogenerated electrons can transfer from PtSe$_2$ into graphene enhanced by the built-in field pointed from graphene to PtSe$_2$. With increasing pump fluence, more electrons transfer into graphene, which indicate more amount of energy has been exchanged between photoexcited carriers and intrinsic conduction band carriers in graphene. The more heated electrons cause larger negative photoconductivity and slower decay time. Under high pump fluence, the photogenerated carriers can partially screen the built-in field, which leads to appearance of both positive and negative THz photoconductivity. By increasing the pump fluence further, the built-in field has been screened completely, which leads to the charge transfer being prevented totally, as a result, only positive THz photoconductivity is observed under high pump

fluence, and the positive THz photoconductivity comes from the response of photocarrier in PtSe$_2$. For the case of G2 heterostructure as schematically illustrated in Fig. 4(b), the substrate induced built-in field is pointed from PtSe$_2$ to graphene, which prevents the charge transfer from PtSe$_2$ to graphene, as a result, the heterostructure behaves PtSe$_2$-like positive THz photoconductivity under various the pump fluences and wavelengths.

Conclusion

In conclusion, the Graphene/5L PtSe$_2$ heterostructures with different stacking orders are fabricated by CVD method, and the ultrafast dynamical charge transfer has been investigated with OPTP spectroscopy. For the G1 heterostructure, the photoconductivity changes from negative to positive with increasing pump fluence, which indicates the carrier injection takes place from PtSe$_2$ into Graphene after photoexcitation. Pump fluence and wavelength dependent transient THz photoconductivity agrees well with the charge transfer model. By contrast, no charge transfer occurs in G2 heterostructure due to the direction of build-in electric field precludes the electron transfer from PtSe$_2$ to graphene. Our experimental results reveal that the built-in electric field induced by silica substrate play a dominated role in the photoinduced charge transfer in Gr/TMDs heterostructure. Our study not only reveals the built-in field is important in Gr/TMDs herterojunction but also certificates an easy way to optimize the optoelectronic response with substrate engineering.

Supplementary Information

The Supporting Information is available free of charge at http://pubs.acs.org /doi/xxxxxxxxxxx.

Absorption and Raman spectra; Transient THz photoconductivity of 5-layer PtSe$_2$ film

References

1.   Wen, X.; Gong, Z.; Li, D., Nonlinear Optics of Two-Dimensional Transition Metal Dichalcogenides. *InfoMat* **2019**, *1*, 317-337.

2.   Sun, Z.; Martinez, A.; Wang, F., Optical Modulators with 2d Layered Materials. *Nature Photon.* **2016**, *10*, 227-238.

3.   Li, L., et al., A General Method for the Chemical Synthesis of Large-Scale, Seamless Transition Metal Dichalcogenide Electronics. *Adv Mater* **2018**, *30*, e1706215.

4.   Liu, Q.; Cook, B.; Gong, M.; Gong, Y.; Ewing, D.; Casper, M.; Stramel, A.; Wu, J., Printable Transfer-Free and Wafer-Size Mos2/Graphene Van Der Waals Heterostructures for High-Performance Photodetection. *ACS Appl Mater Interfaces* **2017**, *9*, 12728-12733.

5.   Kim, Y. C.; Nguyen, V. T.; Lee, S.; Park, J. Y.; Ahn, Y. H., Evaluation of Transport Parameters in Mos2/Graphene Junction Devices Fabricated by Chemical Vapor Deposition. *ACS Appl Mater Interfaces* **2018**, *10*, 5771-5778.

6.   Lin, S., et al., Tunable Active Edge Sites in Ptse2 Films Towards Hydrogen Evolution Reaction. *Nano Energy* **2017**, *42*, 26-33.

7.   Noh, S. H.; Hwang, J.; Kang, J.; Seo, M. H.; Choi, D.; Han, B., Tuning the Catalytic Activity of Heterogeneous Two-Dimensional Transition Metal Dichalcogenides for Hydrogen Evolution. *J. Mater. Chem. A* **2018**, *6*, 20005-20014.

8.   Geim, A. K.; Grigorieva, I. V., Van Der Waals Heterostructures. *Nature* **2013**, *499*, 419-425.

9.   Li, Y.; Zhou, H.; Chen, Y.; Zhao, Y.; Zhu, H., Efficient Hot-Electron Extraction in Two-Dimensional Semiconductor Heterostructures by Ultrafast Resonant Transfer. *J Chem Phys* **2020**, *153*, 044705.

10.   Baranowski, M., et al., Probing the Interlayer Exciton Physics in a Mos2/Mose2/Mos2 Van Der Waals Heterostructure. *Nano Lett* **2017**, *17*, 6360-6365.

11.   Sattar, S.; Schwingenschlogl, U., Electronic Properties of Graphene-Ptse2 Contacts. *ACS Appl Mater Interfaces* **2017**, *9*, 15809-15813.

12.   Bellus, M. Z.; Mahjouri-Samani, M.; Lane, S. D.; Oyedele, A. D.; Li, X.; Puretzky, A. A.; Geohegan, D.; Xiao, K.; Zhao, H., Photocarrier Transfer across Monolayer Mos2-MoSe2 Lateral Heterojunctions. *ACS Nano* **2018**, *12*, 7086-7092.

13.   Zhu, X.; Monahan, N. R.; Gong, Z.; Zhu, H.; Williams, K. W.; Nelson, C. A., Charge Transfer Excitons at Van Der Waals Interfaces. *J Am Chem Soc* **2015**, *137*, 8313-20.

14.   Yuan, L.; Zheng, B.; Kunstmann, J.; Brumme, T.; Kuc, A. B.; Ma, C.; Deng, S.; Blach, D.; Pan, A.; Huang, L., Twist-Angle-Dependent Interlayer Exciton Diffusion in WS2-WSe2 Heterobilayers. *Nat Mater* **2020**, *19*, 617-623.

15.   Chen, H., et al., Ultrafast Formation of Interlayer Hot Excitons in Atomically Thin MoS2/WS2 Heterostructures. *Nat Commun* **2016**, *7*, 12512.

16.   Yuan, L.; Chung, T.; Kuc, A.; Wan, Y.; Xu, Y.; Chen, Y.; Heine, T.; Huang, L., Photocarrier Generation from Interlayer Charge-Transfer Transitions in Ws2-Graphene Heterostructures. *Sci. Adv.*

2018, *4*, 1-9.

17.	Yang, B., et al., Effect of Distance on Photoluminescence Quenching and Proximity-Induced Spin-Orbit Coupling in Graphene/Wse2 Heterostructures. *Nano Lett* **2018**, *18*, 3580-3585.

18.	Fu, S., et al., Long-Lived Charge Separation Following Pump-Energy Dependent Ultrafast Charge Transfer in Graphene/Ws2 Heterostructures. *arXiv:2101.05595* **2020**.

19.	Xing, X.; Zhao, L.; Zhang, W.; Wang, Z.; Su, H.; Chen, H.; Ma, G.; Dai, J.; Zhang, W., Influence of a Substrate on Ultrafast Interfacial Charge Transfer and Dynamical Interlayer Excitons in Monolayer Wse2/Graphene Heterostructures. *Nanoscale* **2020**, *12*, 2498-2506.

20.	Bradac, C.; Xu, Z. Q.; Aharonovich, I., Quantum Energy and Charge Transfer at Two-Dimensional Interfaces. *Nano Lett* **2021**, *21*, 1193-1204.

21.	Chen, Y.; Li, Y.; Zhao, Y.; Zhou, H.; Zhu, H., Highly Efficient Hot Electron Harvesting from Graphene before Electron-Hole Thermalization. *Sci. Adv.* **2019**, *5*, 1-7.

22.	Sun, Y.; Wang, R.; Liu, K., Substrate Induced Changes in Atomically Thin 2-Dimensional Semiconductors: Fundamentals, Engineering, and Applications. *Appl. Phys. Rev* **2017**, *4*.

23.	Yu, Z. G.; Zhang, Y.-W.; Yakobson, B. I., Strain-Robust and Electric Field Tunable Band Alignments in Van Der Waals WSe$_2$–Graphene Heterojunctions. *J. Phys. Chem. C* **2016**, *120*, 22702-22709.

24.	Fu, J., et al., Thickness-Dependent Ultrafast Photocarrier Dynamics in Selenizing Platinum Thin Films. *J. Phys. Chem. C* **2020**, *124*, 10719-10726.

25.	Wang, L., et al., Nonlinear Optical Signatures of the Transition from Semiconductor to Semimetal in PtSe$_2$. *Laser & Photonics Reviews* **2019**, *13*.

26.	Zhang, Z.; Lin, T.; Xing, X.; Lin, X.; Meng, X.; Cheng, Z.; Jin, Z.; Ma, G., Photoexcited Terahertz Conductivity Dynamics of Graphene Tuned by Oxygen-Adsorption. *Appl. Phys. Lett.* **2017**, *110*.

27.	Mics, Z.; Tielrooij, K. J.; Parvez, K.; Jensen, S. A.; Ivanov, I.; Feng, X.; Mullen, K.; Bonn, M.; Turchinovich, D., Thermodynamic Picture of Ultrafast Charge Transport in Graphene. *Nat Commun* **2015**, *6*, 7655.

28.	Ferrari, A. C., et al., Raman Spectrum of Graphene and Graphene Layers. *Phys Rev Lett* **2006**, *97*, 187401.

29.	Xing, X., et al., Photoinduced Terahertz Conductivity and Carrier Relaxation in Thermal-Reduced Multilayer Graphene Oxide Films. *The Journal of Physical Chemistry C* **2017**, *121*, 2451-2458.

30.	Tielrooij, K. J.; Song, J. C. W.; Jensen, S. A.; Centeno, A.; Pesquera, A.; Zurutuza Elorza, A.; Bonn, M.; Levitov, L. S.; Koppens, F. H. L., Photoexcitation Cascade and Multiple Hot-Carrier Generation in Graphene. *Nature Physics* **2013**, *9*, 248-252.

31.	Jensen, S. A.; Mics, Z.; Ivanov, I.; Varol, H. S.; Turchinovich, D.; Koppens, F. H.; Bonn, M.; Tielrooij, K. J., Competing Ultrafast Energy Relaxation Pathways in Photoexcited Graphene. *Nano Lett* **2014**, *14*, 5839-5845.

32.	Mihnev, M. T., et al., Microscopic Origins of the Terahertz Carrier Relaxation and Cooling Dynamics in Graphene. *Nat Commun* **2016**, *7*, 11617.

33.	Sun, M.; Chou, J.-P.; Yu, J.; Tang, W., Effects of Structural Imperfection on the Electronic Properties of Graphene/WSe$_2$ Heterostructures. *J. Mater. Chem. C* **2017**, *5*, 10383-10390.

Hot carrier transfer in graphene/PtSe₂ heterostructure tuned by built-in electric field

Qiushi Ma[1,2], Wenjie Zhang[3], Chunwei Wang[2,4], Ruihua Pu[2], Chengwei Ju[5], Xian Lin[3], Zeyu Zhang[4*], Weiming Liu[2*], and Ruxin Li[2,4]

[1] School of Resource and Environmental Engineering, Hefei University of Technology, Hefei 230009, Anhui Province, China

[2] School of Physical Science and Technology, ShanghaiTech University, Shanghai 201210, China

[3] Department of Physics, Shanghai University, Shanghai 200444, China

[4] State Key Laboratory of High Field Laser Physics and CAS Center for Excellence in Ultra-intense Laser Science, Shanghai Institute of Optics and Fine Mechanics (SIOM), Chinese Academy of Sciences (CAS), Shanghai 201800, China

[5] College of Chemistry, Nankai University, Tianjin 300071, China

*Corresponding Authors, zhangzeyu@siom.ac.cn (Z.Zhang), liuwm@shanghaitech.edu.cn (W. Liu)

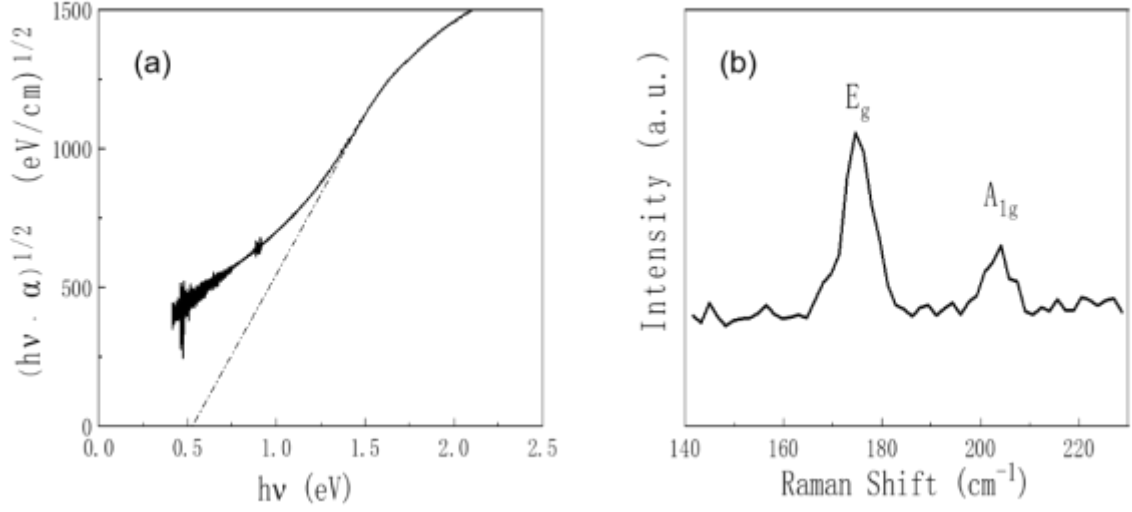1. UV-visible absorption spectrum as well as the Raman spectroscopy of 5-layer PtSe2 film on silica substrate.

Figure S1. (a) Tauc plots of 5-layer PtSe$_2$ film obtained from UV-visible absorption spectrum. (b) Raman scattering spectrum of silica substrate supported 5-layer PtSe$_2$ film.

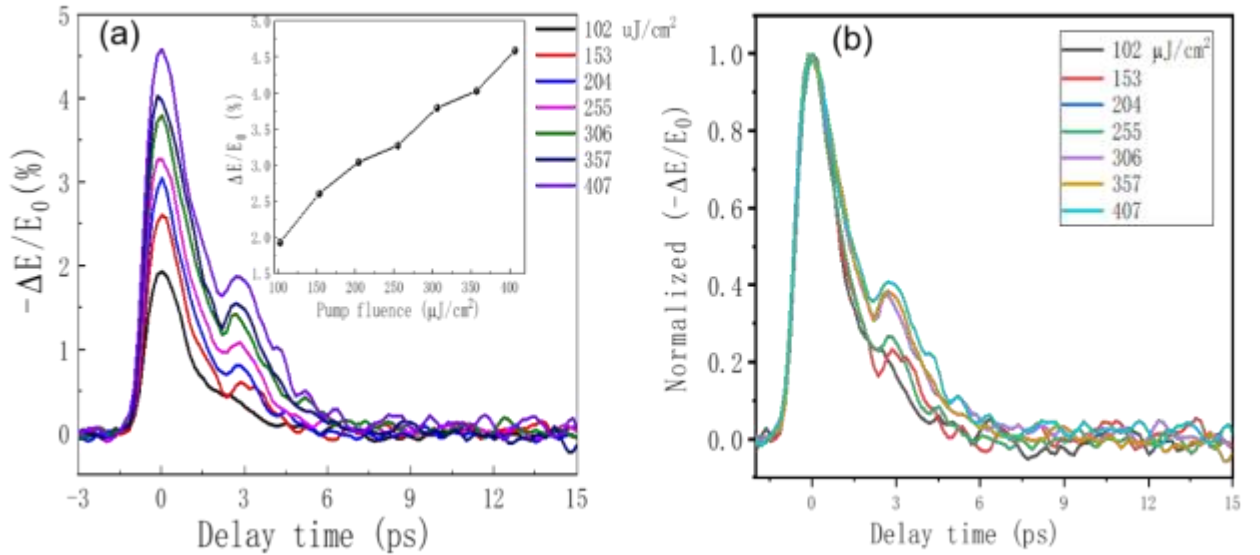## 2. Photoinduced transient THz photoconductivity in 5-layer PtSe$_2$

Figure S2. The transient THz photoconductivity of 5L PtSe$_2$ excited under various pump fluence at

780 nm. The inset plot shows $\Delta E/E_0$ with respect to the pump fluence (b) Normalized THz photoconductivity from (a).